

^{22}Ne a primary source of neutrons for the s-process and a major neutron poison in very metal-poor asymptotic giant branch stars

R. Gallino*, S. Bisterzo and L. Husti

Dipartimento di Fisica Generale, Università di Torino, Via Pietro Giuria 1, 10125 Torino, Italy

E-mail: gallino@ph.unito.it, bisterzo@ph.unito.it, husti@ph.unito.it

F. Käppeler

Forschungszentrum Karlsruhe, Institut für Kernphysik, D-76021 Karlsruhe, Germany

E-mail: franz.kaeppler@ik.fzk.de

S. Cristallo and O. Straniero

INAF - Osservatorio di Teramo (INAF), Teramo, Italy

E-mail: cristallo@oa-teramo.inaf.it, straniero@oa-teramo.inaf.it

In AGB stars of low mass and very low metallicity, $[\text{Fe}/\text{H}] < -2$, a large abundance of primary ^{12}C is mixed with the envelope by each third dredge up episode. The subsequent activation of the H shell converts almost all CNO nuclei into ^{14}N . Thus the H burning ashes contain ^{14}N from the original CNO nuclei, plus an increasing amount of primary ^{14}N . During the subsequent convective thermal instability in the He shell, all the ^{14}N nuclides are converted to ^{22}Ne by $^{14}\text{N}(\alpha, \gamma)^{18}\text{F}(\beta + \nu)^{18}\text{O}$, followed by $^{18}\text{O}(\alpha, \gamma)^{22}\text{Ne}$. At the peak temperature reached at the base of the thermal pulse, the $^{22}\text{Ne}(\alpha, n)^{25}\text{Mg}$ reaction is partly activated, giving rise to a small neutron exposure. At the same time, although the neutron capture cross section of ^{22}Ne is very small ($\sigma(^{22}\text{Ne}, 30\text{keV}) = 0.059 \pm 0.0057$ mbarn, Beer et al. 1991), the very large amount of primary ^{22}Ne acts as a major poison against the s process. This poison effect is substantial also in case of addition of a ^{13}C -pocket. Some fraction of primary ^{16}O is also made in the thermal pulse by α -capture on ^{12}C (with mass fraction $X(^{16}\text{O}) \simeq 0.003$, while $X(^{12}\text{C}) \simeq 0.20$). Besides ^{12}C and ^{22}Ne , a number of light isotopes are largely produced in a primary way, among which one finds ^{19}F (from neutron capture on ^{18}O), ^{23}Na , ^{25}Mg , ^{26}Mg . An effort should be devoted to improve the accuracy of the cross sections of these light isotopes, in order to better constrain the s-process efficiency and their production in low metallicity AGB stars. At very low metallicity, iron is directly made starting from neutron captures on ^{22}Ne and then used as a bridge for the build-up of the s elements.

International Symposium on Nuclear Astrophysics — Nuclei in the Cosmos — IX

June 25-30 2006

CERN, Geneva, Switzerland

* Speaker.

1. Introduction

Large scale stellar surveys provided a sample of carbon enhanced and s-rich metal-poor stars with $[\text{Fe}/\text{H}] < -2$. The observed stars have masses of about $0.8 M_{\odot}$ and they are either on the main sequence, or in the giant phase. The high C and s element abundances observed in these stars are not the result of an intrinsic nucleosynthesis process in the observed star, but of accretion through stellar winds in a binary system from the more massive companion (now a white dwarf) while it was on the Asymptotic Giant Branch (AGB). These objects are classified as extrinsic AGBs.

The AGB structure is characterized by a C-O core and by two alternate H and He burning shells. While the H burning shell progresses outwards, the region containing the ashes of H burning is heated up until He ignites quasi explosively, developing a thermal pulse (TP) that forces the whole region between the H shell and He shell (He intershell) to become convective. During the thermal pulse, a large abundance of ^{12}C is produced by partial He burning. At the quenching of the thermal pulse, the H shell is temporarily inactivated and the bottom of the convective envelope penetrates into the top region of the He intershell, mixing with the surface freshly synthesized ^{12}C and s elements (third dredge up, TDU).

The major neutron source is the $^{13}\text{C}(\alpha, n)^{16}\text{O}$ reaction. During the third dredge up, where the H-rich convective envelope and the He-rich radiative zone get into contact, a small amount of protons is assumed to penetrate from the H-rich envelope into the top layers of the He intershell. At H reignition, these protons are captured by the large abundance of ^{12}C , giving rise to a ^{13}C pocket, via the reaction chain $^{12}\text{C}(p, \gamma)^{13}\text{N}(\beta^+ \nu)^{13}\text{C}$, eventually followed by $^{13}\text{C}(p, \gamma)^{14}\text{N}$ in case some extra protons survive the capture on the abundant ^{12}C . Later on, ^{13}C burns radiatively in the interpulse phase at $T \sim 0.9 \times 10^8$ K, thus releasing neutrons which are used for the build up of s-process elements. The s-rich pocket is then engulfed by the growing convective thermal instability. We consider a large range of ^{13}C pocket efficiencies, as required by the observations of s-enhanced stars at various metallicities (see Busso, Gallino & Wasserburg (1999); Bisterzo et al. 2005; Straniero, Gallino & Cristallo (2006)). The ST case corresponds to a mass pocket of $9.37 \times 10^{-4} M_{\odot}$ containing a total mass of ^{13}C atoms of $4.69 \times 10^{-6} M_{\odot}$ distributed in three subzones. Starting from the top of the pocket, the masses of the three subzones are $7.5 \times 10^{-6} M_{\odot}$, $5.3 \times 10^{-4} M_{\odot}$, and $4.0 \times 10^{-4} M_{\odot}$; each subzone contains a mass fraction $X_{\text{eff}}(^{13}\text{C}) = 1.5 \times 10^{-2}$, 6.37×10^{-3} , and 3.0×10^{-3} , respectively. Here we consider *effective* ^{13}C mass fractions, defined as $X(^{13}\text{C}) - 13/14 X(^{14}\text{N})$. In fact, during the subsequent release of neutrons by the reaction $^{13}\text{C}(\alpha, n)^{16}\text{O}$, any ^{14}N present in the zone would act as a major neutron poison via the resonant reaction $^{14}\text{N}(n, p)^{14}\text{C}$. For a general discussion of the choice of ^{13}C pocket and its profile we refer to Gallino et al. (1998). This ST case was used by Arlandini et al. (1999) and was shown to best reproduce the solar system main component with low mass AGB stellar models of half solar metallicity. Note that small variations in the choice of the ^{13}C pocket, including a finer subzoning, may provide essentially the same s-process distribution.

A second neutron source is provided by the $^{22}\text{Ne}(\alpha, n)^{25}\text{Mg}$ reaction, which is marginally activated during each convective thermal pulse. We study the effect of ^{22}Ne at very low metallicities both as a source of neutrons and as neutron poison for the s process.

2. ^{22}Ne , primary source of neutrons in metal-poor stars

Primary ^{12}C results by partial He burning in the pulse and is mixed with the envelope by previous third dredge up episodes. The H shell transforms all CNO nuclei into ^{14}N , which are then converted by double α -capture to ^{22}Ne during the early development of the next thermal instability. Accordingly, a very large abundance of primary ^{22}Ne is present in the pulse.

We see how ^{22}Ne acts as a source of neutrons in an AGB star of initial mass $1.5 M_{\odot}$ and metallicity $[\text{Fe}/\text{H}] = -2.6$ looking at the no ^{13}C -pocket case of Fig.1 (left panel). In this case, only the ^{22}Ne neutron source is at play. The light-s elements, ls (from Rb to Nb) are enhanced by one order of magnitude, while the production of the heavy-s elements, hs (from Ba to Nd), and of lead, is low. Adding a ^{13}C pocket, a much higher neutron exposure is produced and the effect of ^{22}Ne as a neutron source is overcome. This fact is reflected in the abundances of the s elements shown in Fig.1 (left panel) for the ST \times 2 case, where $[\text{ls}/\text{Fe}] \sim 2.5$ dex, $[\text{hs}/\text{Fe}] \sim 3$ dex, $[\text{Pb}/\text{Fe}] \sim 4.7$ dex. Also for the ST/12 case, $[\text{ls}/\text{Fe}] \sim 2.5$ dex, $[\text{hs}/\text{Fe}] \sim 3$ dex, $[\text{Pb}/\text{Fe}] \sim 3.4$ dex.

For lower metallicities the importance of ^{22}Ne as a neutron source strongly increases. For example, at $[\text{Fe}/\text{H}] = -3.6$, one finds, for the no ^{13}C -pocket case, $[\text{ls}/\text{Fe}] \sim 2.8$ dex, $[\text{hs}/\text{Fe}] \sim 2$ dex, $[\text{Pb}/\text{Fe}] \sim 1.6$ dex. For higher metallicities instead the impact of the of primary ^{22}Ne is strongly diminished, because of the concomitant increase of the Fe seeds and of the light neutron poisons.

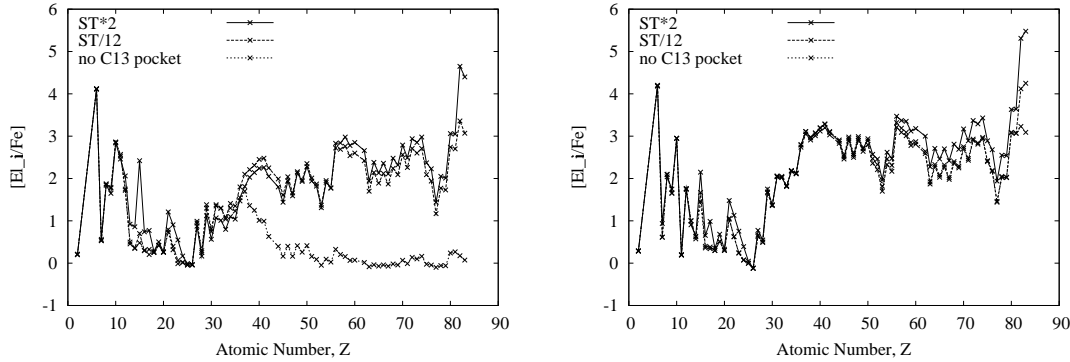


Figure 1: *Left panel* : Element abundance distributions for ST*2, ST/12, and NO ^{13}C pocket of a $1.5M_{\odot}$ star, with $[\text{Fe}/\text{H}] = -2.6$. *Right panel* : Same as the left panel, but for the test case where the $^{22}\text{Ne}(n,\gamma)^{23}\text{Ne}$ cross section is put to zero.

3. ^{22}Ne , major neutron poison

In order to study the effect of ^{22}Ne as a neutron poison we made a test case in which we excluded the $^{22}\text{Ne}(n,\gamma)^{23}\text{Ne}$ channel. This test is unrealistic, but permits to understand how ^{22}Ne affects the production of the s elements. The results for $[\text{Fe}/\text{H}] = -2.6$ are shown in the right panel of Fig.1 (right panel). Putting to zero the neutron capture cross section of ^{22}Ne , for the no ^{13}C pocket case all s elements are strongly overproduced, with $[\text{ls}/\text{Fe}] \sim [\text{hs}/\text{Fe}] \sim [\text{Pb}/\text{Fe}] \sim 3$ dex. A similar effect is also evident in the ST and ST/12 cases. Here, ^{22}Ne acts as neutron poison also in the pocket.

For higher metallicities the importance of the neutron poison effect due to ^{22}Ne decreases. At $[\text{Fe}/\text{H}] = -1$, using a ST ^{13}C pocket the s-process abundance distribution of the test case and the normal one are almost identical.

4. ^{22}Ne cross section uncertainties

In Fig.2 we show the effect of changing by factor of 2 the values of the $^{22}\text{Ne}(n,\gamma)^{23}\text{Ne}$ rate (left panel) or of the $^{22}\text{Ne}(\alpha,n)^{25}\text{Mg}$ rate (right panel). Reducing the $^{22}\text{Ne}(n,\gamma)^{23}\text{Ne}$ cross section by a factor of 2 makes the hs elements increase by about 0.3 dex, while the abundances of the ls elements remain almost unchanged. Using a cross section multiplied by a factor of 2, we observe a decrease by 0.3 dex for both ls and hs elements. These simple tests show how important it is to have precise cross sections for the isotopes that play a major role as poisons for the s process. In the right panel of Fig. 2 we see that changing the $^{22}\text{Ne}(\alpha,n)^{25}\text{Mg}$ rate by a factor of 2 affects especially the light ls elements.

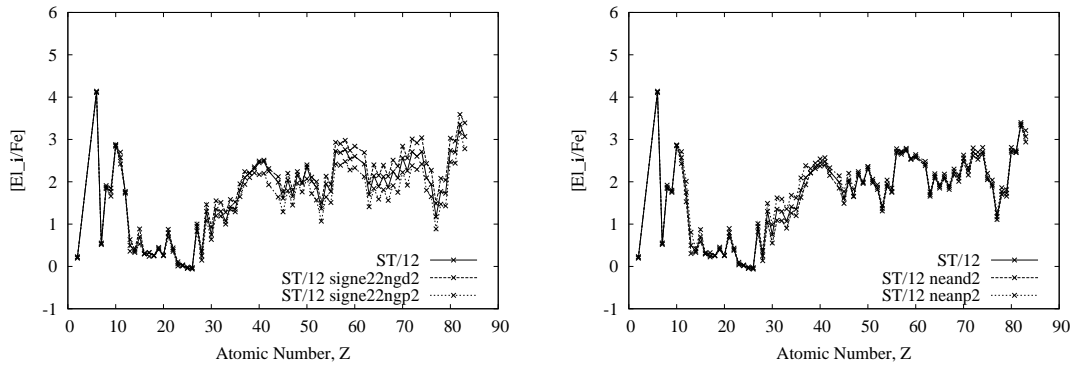


Figure 2: *Left panel* : Element abundance distributions for the ST/12 case of a $1.5M_{\odot}$ star, with $[\text{Fe}/\text{H}]=-2.6$. Solid line stands for a standard $^{22}\text{Ne}(n,\gamma)^{23}\text{Ne}$ cross section, long dashed for the $^{22}\text{Ne}(n,\gamma)^{23}\text{Ne}$ cross section divided by 2 and short dashed for the $^{22}\text{Ne}(n,\gamma)^{23}\text{Ne}$ cross section multiplied by a factor of 2. *Right panel* : Same as the left panel, but for the $^{22}\text{Ne}(\alpha,n)^{25}\text{Mg}$ reaction.

5. The effect of neutron capture on ^{22}Ne for the production of primary light isotopes

Neutron capture acts also on light isotopes producing in different proportions primary ^{19}F , ^{22}Ne , ^{23}Na , ^{24}Mg , ^{25}Mg , ^{26}Mg , ^{27}Al , ^{31}P .

We observe that at $[\text{Fe}/\text{H}] = -2.6$, putting to zero the $^{22}\text{Ne}(n,\gamma)^{23}\text{Ne}$ cross section, the envelope abundance of ^{23}Na decreases drastically, by a factor of 300 to 200 according to the strength of the ^{13}C pocket, while the ^{22}Ne abundance remains unchanged. ^{24}Mg also decreases, by a factor of 3 to 5. Thus, the large primary production of ^{23}Na is a consequence of the neutron capture on primary ^{22}Ne . Note that some primary production of ^{24}Mg derives from neutron captures on ^{23}Na .

6. Primary production of ^{19}F

A special case is ^{19}F , whose envelope abundance is increased by a factor of 50 in our computations. An additional very important contribution to primary ^{19}F and to primary ^{14}N in very

metal-poor stars of $[\text{Fe}/\text{H}] \leq -2.3$ may derive from the occurrence of an anomalous H convective flash followed by a huge first TDU (Hollowell et al. (1990); Fujimoto, Ikeda & Iben (2000); Iwamoto et al. (2004); Straniero et al. (2004)), with a surface $[\text{F}/\text{Fe}] \sim 3$ and $[\text{N}/\text{Fe}] \sim 2$.

7. ^{22}Ne , source of s-process iron, a bridge to the s elements

We demonstrate how in very metal-poor stars the neutron capture chain starting from ^{22}Ne is capable to first produce iron (by neutron captures!) and then all the s elements. In a new test we put to zero the initial abundances of all isotopes from ^{56}Fe up to ^{209}Bi . In Fig.3 we see that for the $\text{ST} \times 2$ case the resulting s-process distribution is almost the same as in the normal case with solar scaled Fe and heavy elements beyond Fe (Fig.1, left panel), whereas for the $\text{ST}/12$ or no ^{13}C -pocket cases a lower s-process efficiency than in the normal case comes out. We have to realise that for very low metallicities and the $\text{ST} \times 2$ case the neutron exposure in the pocket is so intense that the initial abundance of the seed nuclei is unessential.

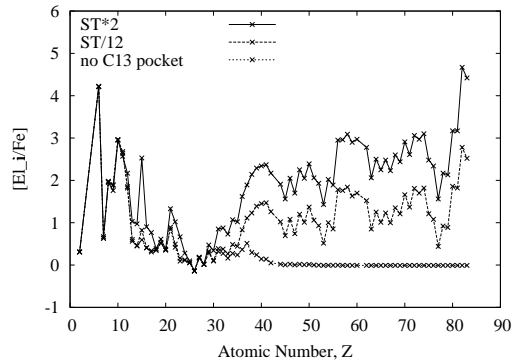


Figure 3: Element abundance distributions of a $1.5M_{\odot}$ star, with $[\text{Fe}/\text{H}] = -2.6$, for the $\text{ST} \times 2$, $\text{ST}/12$, and $\text{NO } ^{13}\text{C}$ pocket with the initial abundance of all isotopes from ^{56}Fe to ^{209}Bi put to zero.

8. Conclusions

^{22}Ne acts as a primary neutron source, independent of the stellar metallicity, but it also acts as a neutron poison, having important effects at $[\text{Fe}/\text{H}] < -2$. ^{22}Ne contributes significantly to the production of primary Na and also to the production of s-process iron that acts as a bridge for the formation of the s elements in very low metallicity stars. We finally recall that the role played by neutron capture on primary ^{22}Ne and its progenies in AGB stars of very low metallicities has been anticipated and partly discussed in a number of works (Goriely & Siess (2001); Chieffi et al. (2001); Siess, Livio & Lattanzio (2002); Herwig (2004); Suda et al. (2004, 2005)).

Acknowledgements. We thank the referee for useful indications to improve the text. Work partly supported by the Italian MIUR-FIRB project *The Astrophysical Origin of the Heavy Elements beyond Fe*.

References

- [1] Arlandini, C., Käppeler, F., Wisshak, K., Gallino, R., Lugaro, M., Busso, 1999, *ApJ*, 525, 886
- [2] Beer, H., Rupp, G., Voss, F., Käppeler, F., 1991, *ApJ*, 379, 420
- [3] Bisterzo, S., Gallino, R., Delaude, L., Straniero, O., Ivans, I.I., 2005, in *IAU Symp. 228, From Lithium to Uranium: Elemental Tracers of Early Cosmic Evolution*, (ed. V. Hill, P. François, F. Primas), (Cambridge: Cambridge University Press), p. 481
- [4] Busso, M., Gallino, R., Wasserburg, G.J., 1999, *Annu. Rev. Astron. Astrophys.* 37, 239
- [5] Chieffi, A., Domínguez, I., Limongi, M., Straniero, O., 2001, *ApJ*, 554, 1159
- [6] Fujimoto, M., Ikeda, Y., Iben, I.Jr, 2000, *ApJ*, 529, L25
- [7] Gallino, R., Arlandini, C., Busso, M., Lugaro, M., Travaglio, C., Straniero, O., Chieffi, A., Limongi, M., 1998, *ApJ*, 497, 388
- [8] Goriely, S., Siess, L., 2001, *A&A*, 378, L25
- [9] Herwig, F., 2004, *ApJS*, 155, 651
- [10] Hollowell, D., Iben, I.Jr, Fujimoto, M. 1990, *ApJ*, 351, 245
- [11] Iwamoto, N., Kajino, T., Mathews, G., Fujimoto, M., Aoki, W., 2004, *ApJ*, 602, 377
- [12] Siess, L., Livio, M., Lattanzio, J. 2002, *ApJ*, 570, 329
- [13] Straniero, O., Cristallo, S., Gallino, R., Domínguez, I., 2004, *Mem. Soc. Astron. It.*, 75, 665
- [14] Straniero, O., Gallino, R., Cristallo, S., 2006, *Nucl. Phys. A*, 777, 311
- [15] Suda, T., Aikawa, M., Nishimura, T., Fujimoto, M.Y., Iben, I. Jr, 2005, *Nucl. Phys. A*, 758, 336
- [16] Suda, T., Aikawa, M., Machida, M.N., Fujimoto, M.Y., Iben, I. Jr, 2004, *ApJ*, 611, 476